Pragya Darsan, 2025, 6(2) *@DEPAN, UCU*
ISSN: 2542-2634 (print) *Research Article*
https://doi.org/10.3126/pdmdj.v6i2.79719

ADSORPTION FREE ENERGY OF BIPHENYL AND ANILINE ON THE SURFACE OF GRAPHENE AT DIFFERENT TEMPERATURES

G. C. Kaphle[1, 2 *], B. P. Bhatta[1], K. R. Bhatta[3], P. Bhujel[3], D. P. Acharya[1], M. KC[1], P. Khadka[3]

[1]Central Department of Physics, T. U., Kirtipur, Kathmandu, Nepal
[2] Material Science and Computational nano lab, CDP, TU, Kathmandu, Nepal
[3]GoldenGate International College, Tribhuvan University, Kathmandu Nepal

[*]*Corresponding Email*: gck223@gmail.com, gopi.kaphle@cdp.tu.edu.np

Received: August 14, 2024 Revised: November 22, 2024 Accepted: December 20, 2024

Abstract

Adsorption free energy is important for the fundamental and practical aspect to describe the nature of the reaction and to understand the interconnection of the various ingredients involved in the adsorption process. It is also useful to understand the thermodynamics of the molecules in drug delivery, removal of contaminant and protein folding among other. Here, we used TIP3P water model as a solvent to find out the adsorption free energy of the biphenyl and aniline on the surface of graphene at different temperatures through NAMD (Nanoscale Molecular Dynamics) for simulations and VMD (Visual Molecular Dynamics) for molecular visualization and modeling of the system. Overall calculations are performed within the framework of Adaptive Biasing Force (ABF) method in different temperatures at 1.03×10^5 Pascal pressure. The value of adsorption free energy of the systems in the NPT ensembles increase as increasing the temperature on both the systems. The calculation reveals that at the surface of graphene, biphenyl has a higher adsorption free energy than aniline. The present calculation for biphenyl is in excellent agreement with the prior result at 300 K.

Keywords: *Energy Diagrams, Force field, Free energy Calculation, Molecular Dynamics, Nanoparticles.*

INTRODUCTION

The study of zero dimensional to three-dimensional nano-materials, as well as their corresponding derivatives, is a major emphasis of the twenty-first century. Carbon derivatives including fullerene, carbon nanotubes, graphene, and graphite have received a lot of attention recently(Kučerka et al., 2015). Among these materials, graphene and gadgets can have a significant impact on how these materials are executed(Allen et al., 2010). Adsorption, utilizing computational methods, has an exceptional propensity to design and optimize the nanomaterial, including graphene, for various applications like the removal of contaminants from a mixture of complex types, delivery of a high load of drugs, and so forth. For that, the system needs a reliable model of nanomaterial surfaces and their potential interactions with pertinent materials and solvents in order to fulfill each of these functions. To perform each of these roles, the system requires a trustworthy model of nanomaterial surfaces and their potential interactions with relevant substances and solvents(Balandin et al., 2008; Gautam Khatri et al., 2024). The use of free energy calculations based on simulations of classical molecular dynamics has increased recently in a number of scientific disciplines, including thermodynamics, molecular recognition, and protein folding. Fundamental chemical quantities like equilibrium constants, solubilities, partition coefficients, and adsorption coefficients are linked to the adsorption free energy within the framework of physical and non-physical conditions(Chipot & Pohorille, 2007). In this study, we look into how the temperature impacts the adsorption of aniline and biphenyl on graphene surface.

Graphene, a carbon allotrope and a derivative of graphite is the wonderful substance, was discovered in 2004. It is a thin, single sheet made of layers of graphite that has been sheared off to create the thinnest and stiffest layer possible. Each layer contains sp^2 hybridized carbon atoms which are arranged in a flat, hexagonal lattice structure that resembles a honeycomb. It is a sheet of one atom thick semiconductor material overlapped valence and conduction bands that contain both holes and electrons as charge carriers. Each carbon atom in graphene is linked to three more carbon atoms, leaving one electron free for electrical conduction. In short, highly mobile π-electrons located above and below the graphene sheet make it a million times higher conducting than copper even in the room temperature(Chand et al., 2021; Comer et al., 2015). Mechanically, it is one of the strongest materials and highly elastic with a tensile strength of 130 gigapascals about 300 times greater than the strongest steel. Young's modulus of graphene is about 1 tera pascals and spring constants in the region of 1-5 Nm^{-1}. It exhibits a breaking strength of 42 Nm^{-1}(Darve & Pohorille, 2001). In addition, the current density of graphene is very high about six orders of magnitude higher than that of copper, and hence shows record thermal conductivity at room temperature is approximately $(4.84 \pm 0.44) \times 10^3$ $Wm^{-1}K^{-1}$ to $(5.30 \pm 0.48) \times 10^3$ $Wm^{-1}K^{-1}$ compared to the graphite of approximately 2000 $Wm^{-1}K^{-1}$. The surface area of graphene is 2630 m^2g^{-1} whereas CNTs have 100 to 1000 m^2g^{-1}. Graphene is very light at a density of 0.77 mg^{-1} i.e. the same size of paper is roughly 1000 times

heavier. Also, it can be said that 1 gm of graphene is enough to cover a whole football ground of standard measurements(Darve et al., 2008; Selvaraj et al., 2021). Graphene is almost transparent and can absorb approximately 2.3 % (i.e. transmit about 97.7 %) of the white light intensity and is independent of the wavelength in the optical domain(Comer et al., 2015). The melting point of the graphene is about 4510 K which is about 250 K greater than that of graphite measured under the same technique(Ermer, 1976).

Biphenyl is an organic aromatic hydrocarbon having the molecular formula $C_6H_5C_6H_5$ or $C_{12}H_{10}$ with a distinctively comical smell that forms colorless crystals at room temperature. It is composed of carbons and hydrogen atoms so is called hydrocarbon. It consists of two benzene rings attached at one point by removing single H-atoms from each and the total number of hydrogens is two less than that of two benzene rings(Gibertini et al., 2010), (Casbarra & Procacci, 2021). It doesn't contain any functional group so it is less reactive. The molecular mass of biphenyl is about 154.2 g/mol and its density is 1.04 g/cm^3. The vapor pressure is 4 Pa at 20 °C, water solubility is 4.45 mg/liter at 20 °C, and specific gravity is 0.991. The melting point is 69.2 °C and the boiling point is 255 °C. Crude oil, coal tar, and natural gas are the main sources of biphenyl and they can be pulled out by the distillation method.

Aniline (benzamine or phenylamine) is an organic aromatic hydrocarbon having the molecular formula $C_6H_5NH_2$ with an unpleasant, rotten fish-like smell. It is an oily, colorless poisonous liquid at room temperature. It is a compound of carbon, hydrogen, and nitrogen. Aniline consists of a benzene ring on which the amino group (i.e. NH_3) is attached by removing a hydrogen atom, one from a phenyl group and the other from the amino group. Aniline is obtained especially by the reduction of nitrobenzene. Aniline contains NH_3 as a functional group with basic in nature yielding salts when reacting with mineral salts. The molecular mass of the aniline is 93.13 gm/mol and the density is 1.02 gm/cm^3. The boiling point and melting point of the aniline are 184 °C and -6.3 °C respectively. Aniline is soluble in the organic compound but slightly soluble in water. The vapor pressure is 0.6 mmHg at 20 °C, the water solubility is 0.036 gm/ml. Aniline is toxic that causes skin diseases. It produces toxic oxide on nitrogen while burning(Hansen & van Gunsteren, 2014; Hénin & Chipot, 2004). It is used for the manufacture of chemical compounds like dyes, photographic chemicals, a chemical used in agriculture, drugs, explosive chemicals, plastics, and rubber chemicals(Kundert & Kortemme, 2019).

THEORY

The free energy additionally called the thermodynamic free energy of a system is the most important thermodynamic quantity which is helpful in the thermodynamics of chemical or thermal processes in science. Free energy is also called helpful work and can be extracted from a closed system. It is a function of the energy of a system and can be determined by subtracting an entropy-temperature term; consequently, it characterizes the capacity for temperature-instigated events to happen within a closed system. The adjustment in free energy is an amount of most extreme work that a thermodynamic system can perform in a process at a constant temperature. The calculation of absolutely free energy required a suitable reference. But we do not have this so, we can never figure out absolute free energy. However, relative free energies can be determined using different computational techniques, and hence determined free energies have physical significance. Through knowledge of this, it is conceivable to build up stable states, their thermodynamic properties, and the phase transitions between states, and it is also possible to deduce how stable states are changed by external conditions or other transformations(Kumar et al., 1992; Lee et al., 2008). Based on transform between different states, the free energy calculation can be recognized into two principal terms; geometrical and alchemical transformations. Calculation of free energy for alchemical transformation uses perturbation and thermodynamic integration strategies(Leenaerts et al., 2013). However, the adaptive bias force strategy has been used in the free energy calculation of geometric transformations.

The thermodynamic free energy can be determined by utilizing the Helmholtz or Gibbs free energy which depends on statistical ensembles. In canonical ensembles (NVT ensemble having constant volume and temperature), the free energy termed is Helmholtz free energy A and, in the isothermal, -isobaric ensemble (NPT ensemble having a constant temperature and pressure), it is termed the Gibbs free energy G (Kumar et al., 1992; Lee et al., 2008). In our work, Gibb's free energy has been calculated as the thermodynamic system at constant NPT. This absorbs heat energy from the reservoir and the work energy expands to make room for it. The change in free energy can be expressed in terms of the partition function, Q as;

$$\Delta A = -\frac{1}{\beta}\ln\frac{Q_2}{Q_1} \qquad \ldots(1)$$

Where, $\beta = \frac{1}{kT}$, k=Boltzmann constant.

In terms of a probability distribution, change in free energy ΔA can be expressed as;

$$\Delta A = -\frac{1}{\beta}\ln\frac{P_2}{P_1} \qquad \ldots(2)$$

Among the different calculation methods to compute the thermodynamic free energy, the Adaptive biasing force (ABF) technique, advanced technology has been used(Kumar et al., 1992; Los et al., 2015).

The Adaptive biasing force method is an advanced form of Umbrella sampling which is used to calculate the free energy along the transition coordinates and can be seen as potential from the average force. In Umbrella sampling, an external potential is applied to allow for the exploration of higher energy configurations and the states that they are separate(Tanaka et al., 2013). This method is based on the formalism of thermodynamic integration as the quantity of the average force is calculated directly and force is integrated to calculate free energy. The efficiency of molecular dynamics simulations is improved by using the ABF method by sampling the potential energy surface ineffectively due to free energy barriers. Due to this, the ABF method is used to compute free energy along the selected reaction coordinate ξ (Dissertation, 2018; Kumar et al., 1992) and is given as;

$$A(\xi) = -\frac{1}{\beta}\ln P_{\xi} + A_0 \qquad \ldots(3)$$

Where, $A(\xi)$ is the free energy of the state at a particular value of ξ, P_{ξ} is the probability density of finding the system at ξ and A_0 is a constant. ABF is a method of reaction coordinate sampling that applies a continuous biasing force, which is tuned during the simulation to evaluate the free energy progressively. Uniform sampling can thus be achieved by the on-the-fly calculation of $A(\xi)$ and the implementation of this information in the form of an external bias. Therefore, this model requires no knowledge about the potential of mean force.

The derivative of the free energy with respect to the reaction coordinate can be represented in terms of configurational averages as;

$$\frac{dA(\xi)}{d\xi} = \left\langle \frac{\partial U(x)}{\partial \xi} - \frac{1}{\beta}\left\langle \frac{\partial \ln|J|}{\partial \xi} \right\rangle \right\rangle_{\xi} = \langle . F_{\xi} \rangle_{\xi} \qquad \ldots(4)$$

Where, $\partial U(x)/\partial \xi$ represents the force exerted on the system derived from potential energy function, $\frac{1}{\beta}\left\langle \frac{\partial \ln|J|}{\partial \xi} \right\rangle$ represents a geometric correction that accounts for the difference in a phase space availability as the reaction coordinate varies, and $|J|$ is the determinant of the Jacobean for the transformation from generalized to Cartesian coordinates. $\langle . F_{\xi} \rangle_{\xi}$ is an average force acting along reaction coordinates and is the derivative of the instantaneous force component(Bong et al., 2020; Los et al., 2015). In this thesis work, we have used this approach to calculate the free energy profile for the interaction between graphene-biphenyl and graphene-aniline.

COMPUTATIONAL DETAILS

Molecular Dynamics simulation is an established classical computational simulation technique to study the structural and dynamical properties of interacting particles. It is one of the best techniques to solve the many-body problem. In the molecular simulation, we prepare a sample by selecting the model system consisting of N-interacting particles to solve Newton's equation of motion for this system until the properties of the system that are no longer change with time i.e. equilibrium state. Newton's equation of the motion for an i^{th} atom can be written as;

$$m_i \frac{\partial^2 r_i}{\partial t^2} = -\nabla U(r) = \mathbf{F_i} \qquad \ldots(5) \quad \text{where, } i = 1, 2, 3, \ldots\ldots, N$$

Here, m_I is mass, r_I is the position of i^{th} atoms. This equation (5) gives the relation between mass, rates of change of position i.e. acceleration, and potential energy experienced by i^{th} particles. The negative of the potential gradient gives the force F_i. Integration of equation (5) gives the trajectory of the system describing the positions, velocities, and accelerations of the particles. Mainly there are four steps in MD simulation: Modeling of the system, Initialization, Force calculation, and Integration of equations of motion. The first step of the MD simulation is the preparation of the model of the system, under consideration. In a model of a system, we specify molecules in terms of parameters like atomic masses, charges, van der Waals radii, force field, etc. The model contains the topology file in which parameters are connected(Storelli et al., 2009). All these parameters are specified in the CHARMM36 force field for now. These force fields show a considerable difference in the strategy of parameter specification but have similar functional forms(Gomes et al., 2002). The pairwise additive potential functions calculate the force fields between each particle. The potential energy functions are derived empirically to describe the atomic interactions in classical force. The effective pairwise additive potentials represent the interaction between atoms and molecules. The interactions are divided into two categories; bonded and non-bonded. Bond length stretching, bond angle vibration, proper dihedrals, and improper dihedral are bonded while Coulomb and LJ interactions are the non-bonded interactions(Zhu et al., 2010). The total potential energy is the sum of the bonded and non-bonded interactions energies which is given by:

$$U_{total} = U_{bond} + U_{angle} + U_{proper} + U_{improper} + U_{LJ} + U_{coulomb} \quad \ldots(6)$$

Simulation Set Up

Our simulation is carried out mainly with graphene, a biphenyl molecule with 2265 molecules of water in the hexagonal box at different temperatures. Fig. 1 is a small patch of multi-layer graphene which is constructed by using the inorganic Builder plugin of NAMD in a regular hexagonal box of dimensions D: 12 (i.e. inside diameter of the box) and Z: 2 (i.e. the height of a box). The multi-layer graphene consists of four layers. The graphene layer consists of 1152 numbers of carbon atoms. Each carbon atom is bonded to three other carbon atoms. There is no number of carbon atoms having less or more than three bonds with other carbon atoms. It means the number of C-atoms having less or more bonds should be zero. Here all the simulations were carried out with the NAMD package where all bonded and non-bonded parameters were specified in accordance with CHARMM36 as force field parameters. We use the ParamChem server to generate the topology and parameter files for biphenyl. Before this all, the structure file that is going to be parameterized is necessary. For this, a file of. Mol^2 format is best because it contains information such as a double bond that is not available in a protein data bank file. There are various ways to construct the. Mol^2 format. In this work, we first obtain the structure file in. Mol format by clicking the 3D button from the ChemSpider database and convert it into. Mol^2 format using software called OpenBabel.

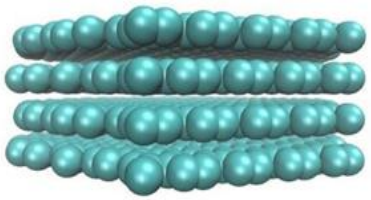

Fig.1: Multilayer Graphene Structure

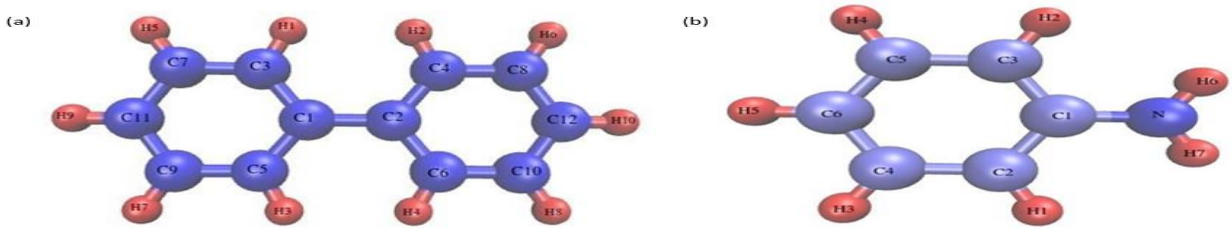

Fig.2.: (a) Structure of biphenyl portrayed by VMD. (b) Structure of aniline portrayed by VMD

Figure 2(a) represents the model of biphenyl with 22 atoms where the bond length and force constant between C-C atoms is 1.3750 Å and 305.00 kcal $mol^{-1}Å^{-2}$ respectively and that of C-H atoms is 1.0900 Å and 340.00 kcal $mol^{-1}Å^{-2}$ respectively. The bond angle and force constant between C-C-C atoms is 120° and 40 kcal $mol^{-1}Å^{-2}$. Similarly, the bond angle and force constant between C-C-H atoms is 120° and 30 kcal $mol^{-1}Å^{-2}$. Figure 2(b) represents the model of aniline with 14 atoms with bond length and force constant between C-C atoms is 1.3750 Å and 305.00 kcal $mol^{-1}Å^{-2}$ respectively, C-H atoms are 1.0900 Å and 340.00 kcal $mol^{-1}Å^{-2}$ respectively, C-N atoms is 1.3900 Å and 400.00 kcal $mol^{-1}Å^{-2}$ respectively and N-H atoms are 1.0000 Å and 488.00 kcal $mol^{-1}Å^{-2}$ respectively.

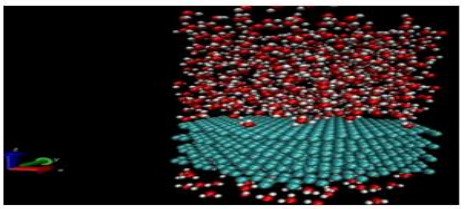

Fig. 3.: Structure of water and graphene

Water molecules to the system containing graphene are added. The water model available for simulation is standard TIP3P (Transferable Intermolecular Potential with 3 points) which is based on the CHARMM36 force field and is widely used in MD simulations of water solvent-solute interactions. It is one of the earliest and most commonly used fixed charges, non-polarizable water model which is implemented in CHARMM force field specifies a three-site rigid water molecule with charges and L-J parameters assigned to each of the three atoms. This model maintains an electrically neutral water molecule has two hydrogen atoms with a partial charge of +0.417e and one oxygen atom carries a partial charge of -0.834e, where e = 1.602×10^{-19} Coulomb. It has a high value of dipole moment of around 2.35 and a dielectric constant of around 82. There are two water models depending upon the flexibility of bond length and angle: rigid TIP3P model and flexible TIP3P model. In the rigid TIP3P model bond length and bond, an angle is fixed while in the flexible TIP3P model bond length and bond angle are changed with time. In this model intramolecular interaction is defined in terms of potentials consisting of harmonic bond stretching and bond angle vibration potentials defined as:

$$U_{OH}(r) = \frac{1}{2}K_{OH}(r - b_{OH})^2 \quad \ldots(7)$$

$$\text{And, } U_{HOH}(\theta) = \frac{1}{2}K_{HOH}(\theta - \theta_0)^2 \quad \ldots(8)$$

Where k_{OH} is the force constant for the bond stretching, b_{OH} is the equilibrium bond length between oxygen and atoms of water. k_{HOH} represents the force constant for bond angle vibration and θ_o represents the equilibrium bond angle HOH. The values of force field parameters for the flexible TIP3P water model are given in the table below;

Table 1.: Force field parameters for the TIP3P water model.

Parameters	Values
K_{OH}	450 kcal $mol^{-1}Å^{-2}$
b_{OH}	0.9572 Å
K_{HOH}	55 kcal mol^{-1} rad^{-2}
θ_0	104.52°

The size of the final system(set of the box) after modeling of water with biphenyl-graphene, and aniline-graphene is (-15 -17 -23) (15 17 23) (i.e. $-15 \leq x \leq 15$Å, $-17 \leq y \leq 17$ Å, and $-23 \leq z \leq 23$ Å) where graphene only is in a range $-15 \leq x \leq 15$ Å x-direction, $-17 \leq y \leq 17$ Å along y-direction and $-15 \leq z \leq -8$ Å along z-direction as shown in fig.4. Now the biphenyl is placed over the graphene and can travel between the surface z 3.5 Å and the bulk aqueous solution z 14 Å many times during the simulation. Before the simulation, make sure that there shouldn't be any water molecules within the graphene layer which may end up stuck between layers of graphene during minimization. If there are, they should be removed before the simulation. Here the total number of atoms is 3439 (22 atoms in biphenyl, 1152 carbon atoms in graphene, and 2265 atoms in water molecules).

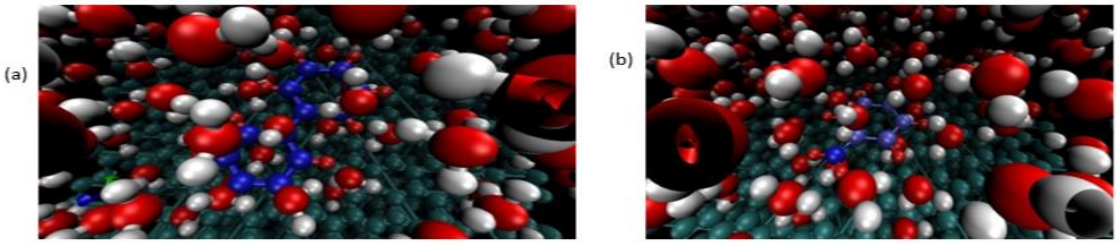

Fig.4.: (a) A system containing biphenyl. (b) System containing aniline ready for simulation portrayed from VMD.

MD simulations were performed using a software package NAMD version 2.12 for Linux-x86 64-multicore. Three-dimensional periodic boundary conditions were applied. The van der Waals and electrostatic interactions were cut-off at 9 Å and the Particle Mesh Ewald (PME) method with a grid spacing of 1.2 Å was used for counting the long-range electrostatic interactions. An isothermal-isobaric (NPT) ensemble was treated. The temperature was controlled by using Langevin force and the pressure was maintained at 1.01325 bar by using the modified Nosé-Hoover method. The system prepared for simulation might contain unphysical Vander Waals contact due to the presence of the atoms which are too close to each other. In this situation, the system does not equilibrate at all and MD fails. To remove this difficulty, we need to carry out energy minimization. The systems were first minimized in energy for 10000 steps to avoid clashes between atoms. This energy-minimized configuration was then used as the initial configuration in the subsequent simulations. After that, the systems were equilibrated at temperatures; 250 K, 260 K, 280 K, 300 K, 320 K, and 340 K for biphenyl and 250 K, 260 K, 280 K, 300 K, 320 K, 350 K for aniline using Langevin dynamics to control the temperature. The Langevin damping coefficient was taken to be 1 ps^{-1}, and the simulations were run for 200 PS with a 2-fs time step and 500000 number steps.

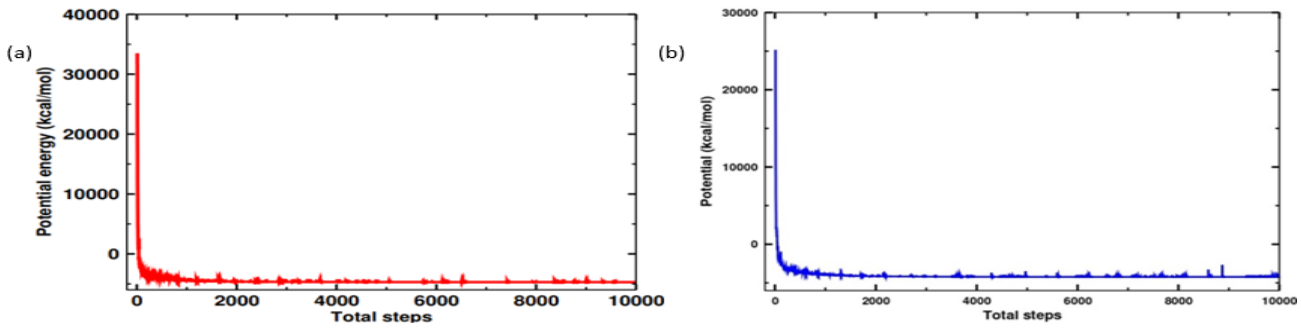

Fig.5. (a) Potential energy after energy minimization for biphenyl (b) Potential energy after energy minimization for aniline at 300 K.

The energy minimization run leads to the situation where the system attains the lowest value of potential energy. After energy minimization, the potential energy of the system containing biphenyl and aniline are shown in figure 5.

Table 2: The temperature fluctuation after the final simulation (a) for biphenyl and (b) for aniline.

(a)

S. N	Coupling Temperature (K)	Average of simulated Temperature (K)
1.	250	249.60± 0.08
2.	260	259.68 ±0.08
3.	280	279.42 ± 0.09
4.	300	299.65 ±0.10
5.	320	319.58 ± 0.10
6.	340	339.64 ±0.11

(b)

S. N	Coupling Temperature (K)	Average of simulated Temperature (K)
1.	250	249.88± 0.08
2.	260	259.50 ±0.08
3.	280	279.54 ± 0.09
4.	300	299.38 ±0.10
5.	320	319.44 ± 0.10
6.	350	349.52 ±0.11

From table 2, it is found that the coupling temperature is almost equal to the average simulated temperature. After equilibration, the system is ready for the final run, the final step of the simulation, which generates the files for calculation of the physical properties of interest. Finally, the system was run at different temperatures for 100 ns with a 2-fs time step and 50000000 number steps. The energy minimization run leads to the situation where the system attains the lowest value of potential energy. The temperature fluctuation after final simulations run for a system containing graphene-biphenyl and graphene-aniline are shown in figure 6.

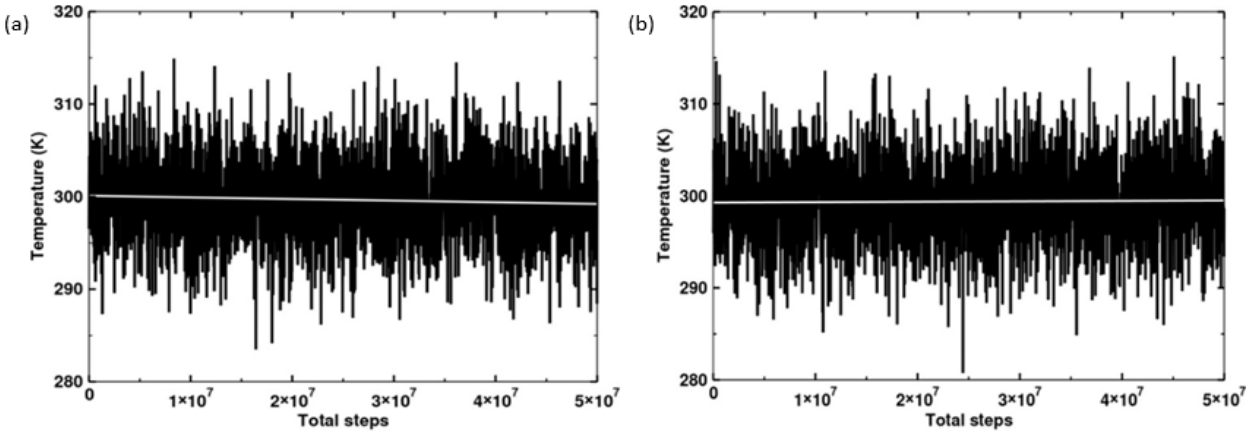

Fig.6. Temperature fluctuation during simulation (a) for biphenyl at 300 K. (b) for aniline at 300 K.

Figure 6 (a) shows the temperature plot of the system containing biphenyl after the final run at 300 K. The average temperature over all the number of steps is 299.65 ± 0.10 K and figure 6 (b) shows the temperature of the system containing aniline at 300 K. The average temperature over all the number of steps is 299.38 ± 0.10 K. The averaged values are represented by a horizontal line in their respective plots.

RESULTS AND DISCUSSION

In this section, we study and analyze the different results of the energy profile and binding energy curve at different temperatures that we have obtained from the simulations.

Energy Profile

The existence of different interactions between atoms gives rise to different energies. The energy profile gives the interaction energy of the system due to bonded and non-bonded interactions. Bonded interactions include bond stretching, bond angle vibration, proper dihedral, and non-bonded interaction includes Van der Waal (Lennard Jones) and Electrostatic interactions. Bonded and non-bonded interaction energies contribute to the potential energy of the system and the total energy of the system is the sum of potential energy and kinetic energy. Energy profiles show manifestations of different temperatures in energy.

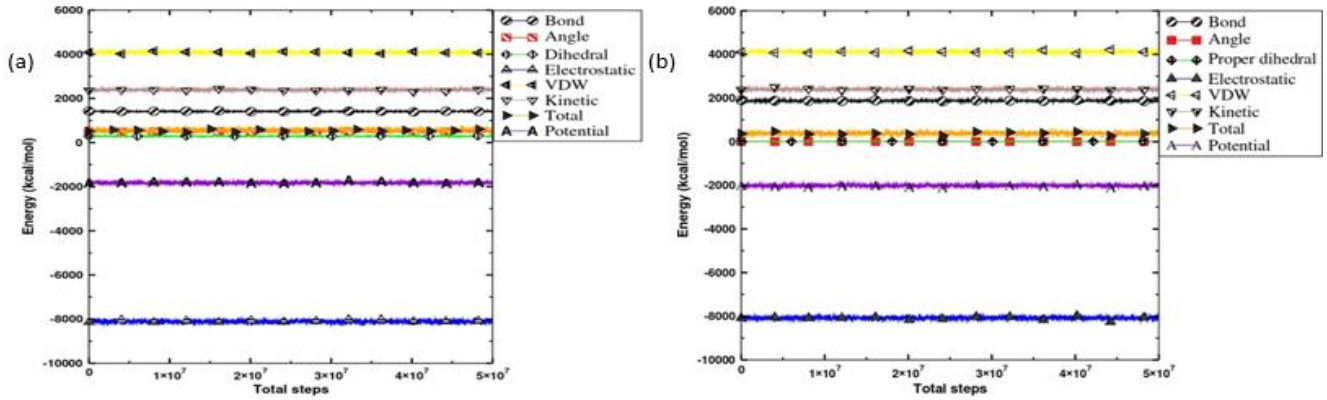

Fig.7. Energy profile of system containing (a) for biphenyl at 300K (b) for aniline at 300K.

The different sorts of energy contributions due to different interactions for the system containing biphenyl and aniline are shown in figure 5 which helps us to compare them with each other. Here Electrostatic potential is negative. The energies due to Electrostatic interaction and L-J interaction have noticeable values and hence contribute significantly to the potential energy. Energies due to angle vibration and dihedral are very less. For aniline, these values are almost coinciding with zero. Energy due to bond stretching also has a noticeable significance to potential energy. The kinetic energy of the system is positive. The potential is negative and larger than kinetic energy in magnitude. Hence total energy is negative which suggests the stability of the system. The relation between kinetic energy and different values of temperature for the system is shown in table 3.

Table 3. The relation between kinetic energy and temperature for the system containing (a) biphenyl and (b) aniline.

(a)

S. N.	Temp. (K)	KE (kcal mol^{-1})	$\frac{KE}{T}$ (kcal mol^{-1} K^{-1})
1.	250	1994.42	7.98
2.	260	2074.98	7.98
3.	280	2232.76	7.97
4.	300	2394.39	7.98
5.	320	2553.64	7.98
6.	340	2713.85	7.98

(b)

S. N.	Temp. (K)	KE (kcal mol^{-1})	$\frac{KE}{T}$ (kcal mol^{-1} K^{-1})
1.	250	1994.45	7.98
2.	260	2068.19	7.95
3.	280	2227.80	7.95
4.	300	2385.97	7.95
5.	320	2545.85	7.95
6.	350	2785.56	7.96

Table 3 shows the ratio of kinetic energy to the corresponding temperature. This ratio is found to be the nearly same for all temperatures for both systems. This value is different for some temperatures for both systems, but the difference is so negligible. Hence, the constant value of the ratio of kinetic energy to temperature gives the relation:

$\frac{KE}{T}$ = a constant $\Rightarrow$ KE = constant × T $\Rightarrow$ KE $\propto$ T. This suggests that the kinetic energy of the system is proportional to the temperature. This is because, at a higher temperature, molecules have higher thermal agitations and hence higher velocity.

Table 4. Different energies of the system containing biphenyl at different temperature

Energy (Kcal/mol)	**250K**	**260K**	**280K**	**300K**	**320K**	**340K**
Bond	1732.43±0.39	1760.87±0.40	1818.21±0.44	1874.69±0.46	1931.48±0.51	1987.89±0.53
Angle	4.72 ± 0.03	4.89 ± 0.03	5.23 ± 0.03	5.54 ± 0.03	5.89 ± 0.04	6.30 ± 0.04
Proper Dihedral	6.81 ± 0.04	7.05 ± 0.04	7.49 ± 0.05	7.87 ± 0.05	8.23 ± 0.05	8.75 ± 0.05
Electrostatic	-8700.90±1.16	-8574.04±1.29	-8323.41±1.26	-8081.67±1.27	-7845.64±1.29	-7614.81±1.38
VDW	4210.42±0.79	4190.59±0.80	4152.35 ±0.81	4117.84±0.84	4087.88±0.82	4059.29±0.85
Potential	-2690.91±0.81	-2553.59±0.87	-2380.20±0.94	-2012.99±0.97	-1746.59±1.05	-1484.12±1.10
Kinetic	1994.42±1.63	2074.98±0.65	2232.76 ±0.70	2394.39±0.74	2553.64±0.79	2713.85±0.86
Total Energy	-696.49±1.04	-478.61±1.10	-47.44 ± 1.18	381.40 ± 1.24	807.05 ± 1.31	1229.73 ± 1.41

Table 5. Different energies of the system containing aniline at different temperature

Energy (Kcal/mol)	250K	260K	280K	300K	320K	350K
Bond	1337.39±0.22	1351.61±0.23	1380.92±0.24	1410.45±0.26	1439.40±0.29	1483.02±0.31
Angle	444.01 ± 0.17	453.67 ± 0.17	474.27 ± 0.19	494.31 ± 0.20	514.38 ± 0.22	544.62 ± 0.23
Proper Dihedral	237.55 ± 0.20	247.23 ± 0.21	265.69 ± 0.22	284.99 ± 0.24	303.22 ± 0.25	332.24 ± 0.28
Electrostatic	-8732.96±1.16	-8605.72±1.19	-8356.08±1.21	-8113.14±1.28	-7880.40±1.33	-7536.54±1.39
VDW	4188.99±0.77	4168.06±0.78	4127.15±0.78	4089.01±0.82	4057.00±0.81	4011.64±0.82
Potential	-2517.36±0.83	-2377.34±0.87	-2099.71±0.94	-1825.54±0.98	-1557.12±1.06	-1155.02±1.14
Kinetic	1991.45±0.63	2068.18±0.63	2227.80±0.71	2385.97±0.76	2545.85±0.80	2785.56±0.87
Total Energy	-525.91±1.05	-309.15±1.06	128.09±1.20	560.43±1.24	988.73±1.32	1630.54±1.42

Table 4 and Table 5 show all types of energies of the system for biphenyl and aniline. There exist various contributions to the potential energy of the system. The sum of all such interactions' potential is the total potential energy. From the above tables, we can see that the potential energy due to bonded interactions increases with temperature but are very small in comparison to other energies. The potential energy due to non-bonded interactions also decreases in magnitude with temperature. The potential energy of the system decreases in magnitude with increasing temperature. The kinetic energy and total energy increase appreciably with temperature. Overall, the values of bond stretching, angle stretching, proper dihedral, VDW, and kinetic energies are positive while Coulomb energy and potential energy are negative.

Free Energy Curve:

The free energy also called the thermodynamic free energy of a system is the most important thermodynamic quantity which is useful in the thermodynamics of chemical or thermal processes in science. Free energy is the useful work that may be extracted from a closed system. It is a function of the energy of a system, subtracted by an entropy-temperature term, thus it defines the capacity for temperature induced events to occur within a closed system. In this work, we performed a free energy calculation as a function of the distance between a center of mass and the plane passing through the centers of the carbon atoms in the first layer of graphene. Free energy may be positive, negative, or zero.

(i) Biphenyl

Figure 8(a) is the free energy profile for biphenyl on the surface of graphene at 300 K. The first minimum is seen at 3.55 Å and the second minimum is at 6.25 Å which is -1.62 kcal mol^{-1}. The maximum depth of the free energy well is -8.16 kcal mol^{-1} at 3.55Å. Thus, the adsorption free energy at 300 K is -8.16 kcal mol^{-1}.

Table 6: Free energy of biphenyl on graphene

S. N.	Temperature (K)	Free Energy (kcal mol^{-1})	Comer et al. (kcal mol^{-1})	Error (%)
1.	250	-7.07	-	-
2.	260	-7.66	-	-
3.	280	-7.77	-	-
4.	300	-8.16	-7.99	2.13
5.	320	-8.75	-	-
6.	340	-8.88	-	-

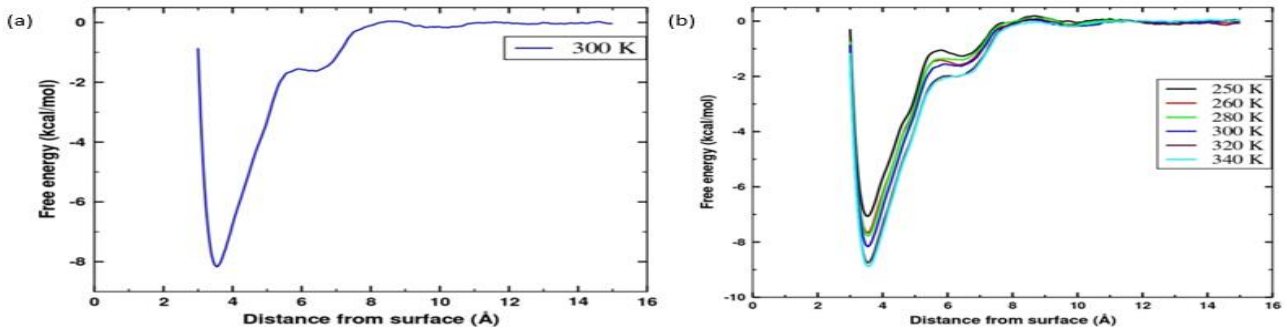

Figure 8.: (a) Adsorption free energy of biphenyl on graphene at 300 K. (b) Adsorption free energy of biphenyl at different temperatures.

(ii) Aniline

Figure 9(a) is the free energy profile for aniline on the surface of graphene at 300 K. The first minimum is seen at 3.50 Å. The maximum depth of the free energy well is -4.26 kcal mol^{-1} at 3.50 Å. Thus, the adsorption free energy at 300 K is -4.26 kcal mol^{-1}. The adsorption free energy of aniline at different temperatures is shown in figure 9(b). Here, we can see that at a distance z = 3.0 Å there is no effect of the adsorption of aniline on graphene and for all temperatures the depth of the free energy curve i.e., the value of free energy is increasing at a distance $z \geq 3.0$ and is maximum at 3.50 Å. The corresponding value of maximum depth gives adsorption free energy. Here we can see that the adsorption free energy of the aniline increases with increasing temperature. For all temperatures, at the distance z = 13.5 Å, the interaction between the graphene and aniline becomes negligible, giving a plateau like at a fixed value, which tends to zero. The value of adsorption free energy of aniline on graphene at different temperatures are given in table 7.

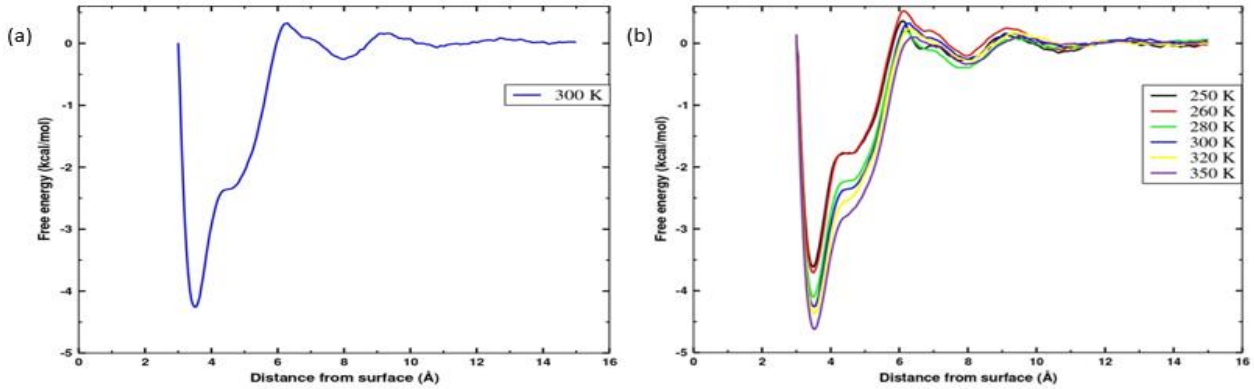

Figure 10.: (a) Adsorption free energy of aniline on graphene at 300 K. (b) Adsorption free energy of aniline at different temperatures

Table 7: Free energy of aniline on graphene

S. N.	Temperature (K)	Free Energy (kcal mol^{-1})
1.	250	-3.62
2.	260	-3.71
3.	280	-4.10
4.	300	-4.26
5.	320	-4.37
6.	340	-4.62

CONCLUSION AND CONCLUDING REMARKS

In our present work, Molecular Dynamics simulations of the system containing biphenyl and aniline as solutes and water as solvents were carried out. Classical Molecular Dynamics simulations were done using NAMD 2.12 for Linux-x86_64-multicores and

CHARMM36 as a force field. VMD version 1.9.3 for LINUXAMD64, (November 30, 2016) is used to design, molecular visualization, modeling, and analyzing the system. We analyzed all the obtained data by xmgrace. During the entire work 2265 water molecules of the TIP3P model, multi-layer graphene (four layers) consisting of 1152 numbers of carbon atoms are used. We calculated the adsorption free energy of the systems containing biphenyl-graphene, aniline-graphene, and water at different temperatures. The pressure for all temperatures was maintained at 1.01×10^5 Pascal by Langevin piston methods. The area of the system was fixed in XY-plane, and the Langevin piston acted along the z-direction only. Bonded interactions (bond, angle, and dihedral) and non-bonded interactions (VDW and electrostatic) were taken into account. Minimization was done for 10000 steps, equilibration was done for 200 PS, and production runs for 100 ns (50000000 steps) using an NPT ensemble. Adsorption free energy was calculated by using Adaptive Biasing Force (ABF) method and results for the biphenyl-graphene system were compared with previous works. The comparison shows a good agreement with previous work with a small deviation of 2.13 % at 300 K for the system containing biphenyl-graphene.

ACKNOWLEDGEMENT

We express our sincere gratitude to the Central Department of Physics, Tribhuvan University.

REFERENCES

Allen, M. J., Tung, V. C., & Kaner, R. B. (2010). Honeycomb Carbon: A Review of Graphene. *Chemical Reviews*, *110*(1), 132–145. https://doi.org/10.1021/cr900070d

Balandin, A. A., Ghosh, S., Bao, W., Calizo, I., Teweldebrhan, D., Miao, F., & Lau, C. N. (2008). Superior Thermal Conductivity of Single-Layer Graphene. *Nano Letters*, *8*(3), 902–907. https://doi.org/10.1021/nl0731872

Bong, A. M., Kor, N. M., & Ndifon, P. T. (2020). Cameroon Green Energy Potentials: Field Survey of Production, Physico-Chemical Analyses of Palm Kernel Oil for Industrial Applications. *Green and Sustainable Chemistry*, *10*(03), 57–71. https://doi.org/10.4236/gsc.2020.103005

Casbarra, L., & Procacci, P. (2021). Binding free energy predictions in host-guest systems using Autodock4. A retrospective analysis on SAMPL6, SAMPL7 and SAMPL8 challenges. *Journal of Computer-Aided Molecular Design*, *35*(6), 721–729. https://doi.org/10.1007/s10822-021-00388-4

Chand, A., Chand, P., Khatri, G. G., & Paudel, D. R. (2021). Enhanced Removal Efficiency of Arsenic and Copper from Aqueous Solution Using Activated Acorus calamus Based Adsorbent. *Chemical and Biochemical Engineering Quarterly*, *3*. https://doi.org/10.15255/CABEQ.2021.1943

Chipot, C., & Pohorille, A. (Eds.). (2007). *Free Energy Calculations* (Vol. 86). Springer Berlin Heidelberg. https://doi.org/10.1007/978-3-540-38448-9

Comer, J., Chen, R., Poblete, H., Vergara-Jaque, A., & Riviere, J. E. (2015). Predicting Adsorption Affinities of Small Molecules on Carbon Nanotubes Using Molecular Dynamics Simulation. *ACS Nano*, *9*(12), 11761–11774. https://doi.org/10.1021/acsnano.5b03592

Darve, E., & Pohorille, A. (2001). Calculating free energies using average force. *The Journal of Chemical Physics*, *115*(20), 9169–9183. https://doi.org/10.1063/1.1410978

Darve, E., Rodríguez-Gómez, D., & Pohorille, A. (2008). Adaptive biasing force method for scalar and vector free energy calculations. *The Journal of Chemical Physics*, *128*(14). https://doi.org/10.1063/1.2829861

Dissertation, A. (2018). *A MOLECULAR DYNAMICS STUDY OF DIFFUSION OF WATER THROUGH CARBON NANOTUBES*.

Ermer, O. (1976). *Calculation of molecular properties using force fields. Applications in organic chemistry* (pp. 161–211). https://doi.org/10.1007/3-540-07671-9_3

Gautam Khatri, G., Baskota, M., Chand, A., Bharati, S., & Paudel, D. R. (2024). Biosorption sudy of Cr (VI) from the aqueous solution using chemically modified biomass of a newly isolated edible mushroom waste. *BIBECHANA*, *21*(3), 221–232. https://doi.org/10.3126/bibechana.v21i3.62097

Gibertini, M., Tomadin, A., Polini, M., Fasolino, A., & Katsnelson, M. I. (2010). Electron density distribution and screening in rippled graphene sheets. *Physical Review B*, *81*(12), 125437. https://doi.org/10.1103/PhysRevB.81.125437

Gomes, R., Meek, M. E., & Eggleton, M. (2002). Concise International Chemical Assessment Document 43: Acrolein. *IPCS Concise International Chemical Assessment Documents*, *43*.

Hansen, N., & van Gunsteren, W. F. (2014). Practical Aspects of Free-Energy Calculations: A Review. *Journal of Chemical Theory and Computation*, *10*(7), 2632–2647. https://doi.org/10.1021/ct500161f

Hénin, J., & Chipot, C. (2004). Overcoming free energy barriers using unconstrained molecular dynamics simulations. *The Journal of Chemical Physics*, *121*(7), 2904–2914. https://doi.org/10.1063/1.1773132

Kučerka, N., van Oosten, B., Pan, J., Heberle, F. A., Harroun, T. A., & Katsaras, J. (2015). Molecular Structures of Fluid Phosphatidylethanolamine Bilayers Obtained from Simulation-to-Experiment Comparisons and Experimental Scattering Density Profiles. *The Journal of Physical Chemistry B*, *119*(5), 1947–1956. https://doi.org/10.1021/jp511159q

Kumar, S., Rosenberg, J. M., Bouzida, D., Swendsen, R. H., & Kollman, P. A. (1992). THE weighted histogram analysis method for free-energy calculations on biomolecules. I. The method. *Journal of Computational Chemistry*, *13*(8), 1011–1021. https://doi.org/10.1002/jcc.540130812

Kundert, K., & Kortemme, T. (2019). Computational design of structured loops for new protein functions. *Biological Chemistry*, *400*(3), 275–288. https://doi.org/10.1515/hsz-2018-0348

Lee, C., Wei, X., Kysar, J. W., & Hone, J. (2008). Measurement of the Elastic Properties and Intrinsic Strength of Monolayer Graphene. *Science*, *321*(5887), 385–388. https://doi.org/10.1126/science.1157996

Leenaerts, O., Partoens, B., & Peeters, F. M. (2013). Adsorption of Molecules on Graphene. In *Graphene Chemistry* (pp. 209–231). Wiley. https://doi.org/10.1002/9781118691281.ch10

Los, J. H., Zakharchenko, K. V., Katsnelson, M. I., & Fasolino, A. (2015). Melting temperature of graphene. *Physical Review B*, *91*(4), 045415. https://doi.org/10.1103/PhysRevB.91.045415

Selvaraj, K., Vishvanathan, N., & Dhandapani, R. (2021). Screening, optimization and characterization of poly hydroxy butyrate from fresh water microalgal isolates. *International Journal of Biobased Plastics*, *3*(1), 139–162. https://doi.org/10.1080/24759651.2021.1926621

Storelli, M. M., Storelli, A., Barone, G., & Franchini, D. (2009). Accumulation of polychlorinated biphenyls and organochlorine pesticide in pet cats and dogs: Assessment of toxicological status. *Science of The Total Environment*, *408*(1), 64–68. https://doi.org/10.1016/j.scitotenv.2009.09.018

Tanaka, A., Nishino, Y., Sakaguchi, S., Yoshikawa, T., Imamura, K., Hashimoto, K., & Kominami, H. (2013). Functionalization of a plasmonic Au/TiO2 photocatalyst with an Ag co-catalyst for quantitative reduction of nitrobenzene to aniline in 2-propanol suspensions under irradiation of visible light. *Chemical Communications*, *49*(25), 2551. https://doi.org/10.1039/c3cc39096a

Zhu, Y., Murali, S., Cai, W., Li, X., Suk, J. W., Potts, J. R., & Ruoff, R. S. (2010). Graphene and Graphene Oxide: Synthesis, Properties, and Applications. *Advanced Materials*, *22*(35), 3906–3924. https://doi.org/10.1002/adma.201001068